ISBN: 978-3-95450-231-8 ISSN: 2673-5490 doi: 10.18429/JACoW-IPAC2023-THPM084

START-TO-END TRACKING OF THERAPEUTIC ION BEAMS IN BDSIM

W. Shields*, John Adams Institute at Royal Holloway, University of London, Egham, UK
S. T. Boogert, Cockcroft Institute, Daresbury, UK
L. J. Nevay, CERN 1211 Meyrin, Switzerland

Abstract

BDSIM is a Monte Carlo simulation program for start-to-end particle tracking through 3D models of particles accelerators. Based on the Geant4 toolkit, BDSIM provides a holistic approach to accelerator modelling by using Geant4's particle-matter interaction physics with dedicated accelerator tracking routines for beam vacuum transport. Subsequently, the ability to model the hits, losses, & energy deposition throughout a machine makes BDSIM highly suited for modelling medical accelerators where beam transmission, target dosimetry, and shielding requirements often need to be considered simultaneously. This has already been demonstrated by BDSIM's adoption in modelling proton therapy beam lines. The growing recognition of ions as a treatment modality that offers a potentially significant improvement in relative biological effectiveness is driving an increase in the number of planned carbon ion therapy centres. The technology to deliver ion beams, however, is prohibitively expensive and remains a challenging research topic. Here, we show the first demonstrations of therapeutic ion tracking in BDSIM in an example model developed for showcasing BDSIM's medical accelerators simulation capabilities.

MODELLING ION THERAPY ACCELERATORS

Cancer treatment is one of the largest medical challenges facing society today. 14.1 million new cases of cancer were reported in 2012, with the rates projected to increase to 24.6 million by 2030 [1]. A number of treatment modalities are employed, with radiotherapy used in ≈ 27% of treatments in the UK [2]. It is estimated, however, that 50% of all cancer patients can benefit from radiotherapy, either as the primary treatment source or in conjunction with other modalities [3].

In recent years, ion therapy had been used particularly for radio-resistant and deep-seated tumours. Similar to protons, ion therapy doses are deposited according to a Bragg peak, however, the lateral and distal fall-offs for ions are sharper, offering improved dose conformality [4]. Ions also offer an increased relative biological effectiveness (RBE) [5], up to 2-3 times the accepted proton RBE of 1.1 [6]. Cost effective ion therapy accelerator technologies, however, remain an ongoing challenge; the higher magnetic rigidity of ions requires larger accelerators and gantries compared to proton therapy systems [7].

A feature of ion therapy is the fragmentation the ions can undergo where the primary ion splits into lighter ions or individual nucleons. This degrades localisation of the delivered dose, with the fragments and other secondary particles depositing their energy beyond the Bragg peak, leading to a characteristic distal tail [8]. Such physics processes can also occur when particles are lost during beam line transport. These losses can result in a large secondary particle flux for which shielding studies may be required for machine protection or background radiation dose evaluation if losses are in close proximity to the gantry isocentre. Modelling these processes in ion therapy accelerators is therefore crucial for understanding not only beam transport performance, but also easily identifying regions of interest where further detailed studies are needed.

BDSIM is a Monte Carlo particle tracking tool for modelling energy deposition in a particle accelerator [9]. Based on the Geant4 toolkit [10], BDSIM combines Geant4's geometry and particle-matter interaction modelling with common accelerator physics matrix tracking routines, providing rapid & accurate dosimetry in full 3D models of particle accelerators. These capapabilities are particularly suited to modelling of medical accelerators where beam characteristics, particles losses, radiation shielding, and dose delivery are often coupled and require simultaneous consideration. BDSIM has already successfully modelled a number of proton therapy accelerators and research facilities [11–14]. To showcase BDSIM's medical accelerator modelling capabilities, an in-house model has also been developed. Previously shown to successfully model protons [15], here we demonstrate the same model but instead tracking ions, highlighting the necessity to not only model the primary ions, but also any secondary particles that are produced.

IN-HOUSE MODEL

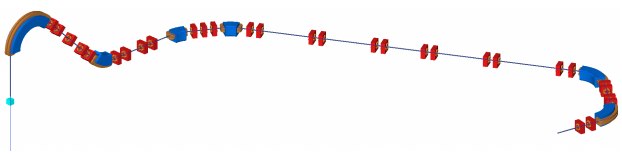

Figure 1: The in-house medical accelerator model in BDSIM based on an early iteration of the PSI gantry 2 bean line.

The in-house model for showcasing medical functionality in BDSIM is based on an early design iteration of Gantry 2 at PSI [16]. The original description of the model in TRANSPORT can be found in [17]. A screenshot of the model's geometry as visualised in BDSIM can be seen in Fig. 1. Originally designed for protons, the converted model contains a degrader for energy selection, however such systems are not used in ion therapy accelerators due to the aforementioned fragmentation processes. To consider this model for ions, we discard the start of the beam line up to

* william.shields@rhul.ac.uk

ISBN: 978-3-95450-231-8 ISSN: 2673-5490 doi: 10.18429/JACoW-IPAC2023-THPM084

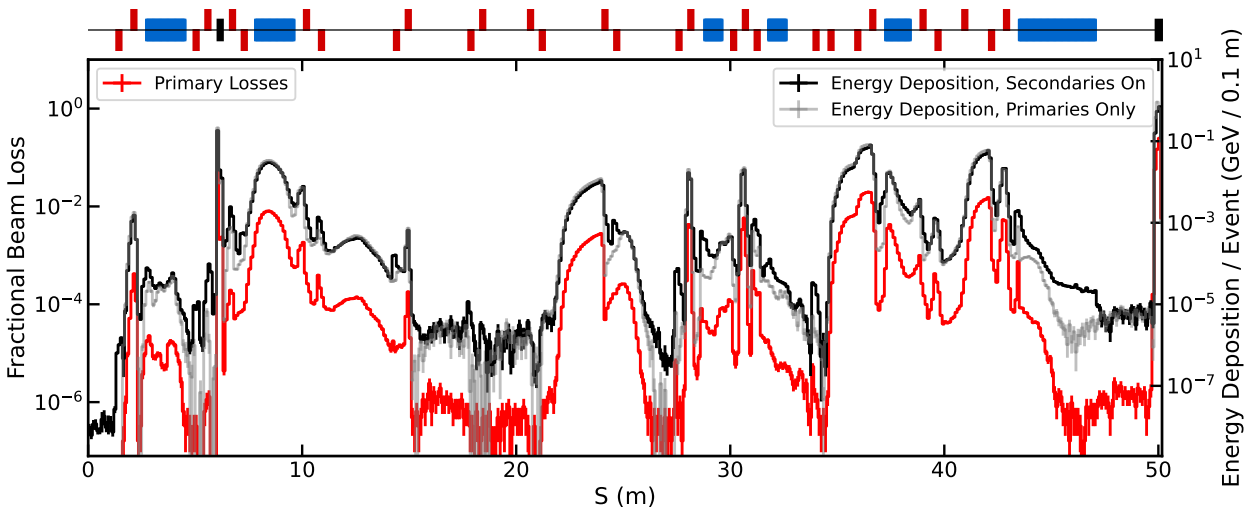

Figure 2: Map of primary particle losses and subsequent energy deposition per event with and without consideration of secondary particle production.

the degrader exit. We preserve the beam parameters at this location; whilst these would have originated from a post-degrader collimators, they are not unreasonable for an ion therapy beam line. A $30 \times 30 \times 30$ *cm* water phantom is also positioned at the gantry isocentre. The primary particle modelled here is carbon-12 ions, the most commonly used ion therapy species, with a total ion kinetic energy of 4.2 GeV corresponding to 350 MeV per nucleon.

TRACKING PERFORMANCE

Whilst the default BDSIM output is a loss map such at that in Fig. 2, BDSIM's tracking performance is first validated by comparison to PTC [18], an independent particle tracking code available through MADX [19]. As the beam grows large at a number of locations along the beam line, the beam pipe aperture is widened to 20 cm diameter to reduce particle losses. The beam pipe is set to be an infinite absorber to prevent lost particles being recaptured downstream. 10000 ^{12}C ions are modelled, with no physicslist defined to restrict the simulations purely to tracking. Thin sampler planes are defined after every lattice element to record all appropriate information of particles at those locations. Whilst the original model represents transport from the final gantry dipole to the isocentre with drift tubes, the length of these drifts are slightly reduced to ensure the centre of the phantom lies at the isocentre. The final 15 cm of drift length is switched to a gap to represent the short air gap between the gantry end and the phantom.

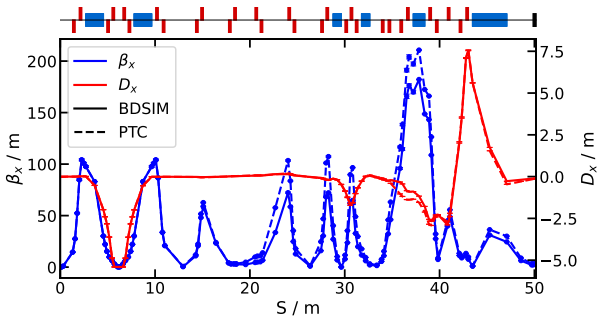

Figure 3: Comparison of the horizontal Twiss β and dispersion functions in BDSIM and PTC for the in-house model set to track ^{12}C ions at kinetic energies of 350 MeV/nucleon.

The horizontal Twiss β and dispersion functions are shown in Fig. 3. Good agreement is observed between the two codes. Differences can be attributed to small differences in loss locations along the beam line. Crucially, good agreement is observed at the gantry isocentre. Although not shown, similar agreement is observed in the vertical plane.

LOSSES & DOSIMETRY

With losses observed in wide aperture tracking-only simulations, further losses are anticipated with nominal beam pipe dimensions. No aperture information was available with the original model, therefore we assume a beam pipe radius of 5 cm. To induce more particle-matter interactions, a 0.25 m long iron collimator replaces the equivalent drift tube length at $S \approx 6.05$ m where β is small and dispersion is large, an ideal location for a momentum cleaning collimator. The collimator aperture is set to 2σ of the beam's nominal spatial dimension at that position. Two simulations were run, one with secondary particle production on, the other off. 1×10^7 primary ions were tracked in both simulations using the QGSP_BIC_EMZ physicslist. The same seeds are used in both simulations to ensure identical initial conditions. These simulations were performed with Geant4-11.0.2.

The per-event primary particle loss locations and subsequent energy deposition are shown in Fig. 2. Whilst the energy deposition broadly agrees between the two simula-

ISBN: 978-3-95450-231-8 ISSN: 2673-5490 doi: 10.18429/JACoW-IPAC2023-THPM084

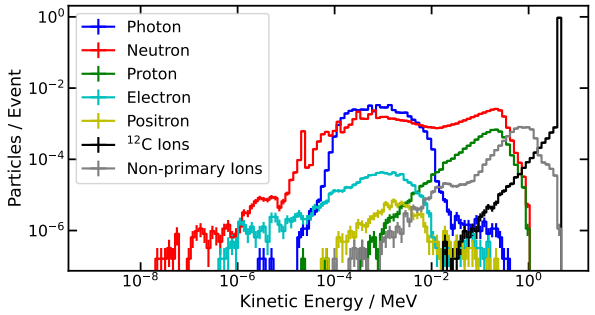

Figure 4: Spectrum of primary ^{12}C ions and all secondary particle species at the exit of the momentum cleaning collimator at S=6 m.

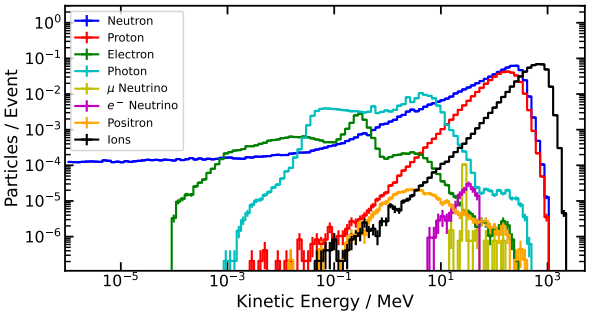

Figure 6: Spectrum of all secondary particles exiting the rear surface of a 30 cm^3 water phantom irradiated with a 350 MeV/u carbon-12 beam.

tions, there are clearly regions that differ, notably within the final gantry dipole. Such differences highlight an increased flux of secondary particles which is crucial to understand given it's proximity to the isocentre.

Differences are also observed around the energy selection collimator. When inspecting the spectra of particles at the collimator exit, Fig. 4 shows a large number of particle species generated. All secondary ions are summed together due to the large number of ion species & isotopes generated. Whilst the primary carbon beam remains the most prominent, a notable low energy tail has been generated. A neutron flux is also present, indicating that subsequent activation studies would be beneficial to ensure safe accelerator operation.

Water Phantom Dose Delivery

The horizontal distribution of primary & secondary particle flux at the gantry exit, phantom entrance, and phantom exit is shown in Fig. 5. Whilst a wide distribution of secondaries is present at the gantry exit, it is acknowledged that the nozzle that would normally occupy this machine region will greatly impact the particle distribution leaving the gantry. What is clear, however, is that there is a significant growth in secondary particle flux resulting from interactions with air in the gap between the final drift & the phantom. The horizontal profile also grows beyond the extent of the 20 cm

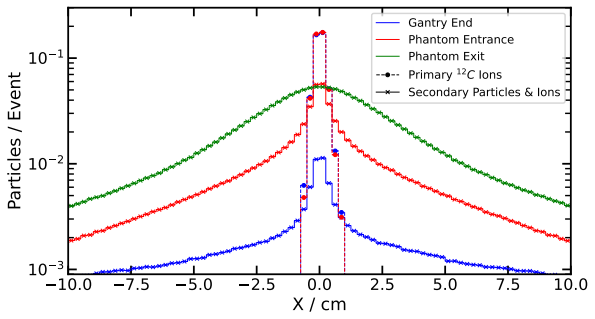

Figure 5: Horizontal distribution of primary and secondary particles at the gantry exit, water phantom entrance, and phantom exit.

wide samplers. Whilst this particle flux does not account for the secondary particle spectrum, modelling it's origin and transport to the phantom is crucial for understanding the background dose delivered to the target volume.

The flux after the phantom is larger still; ion fragments and low energy secondaries produced from particle collisions continue beyond the Bragg peak location, with the characteristic ion dose distal tail extending sufficently far that particles exit the far side of the phantom. When observing the per-event spectrum of this flux, as shown in Fig. 6, it is clear that a large flux of ions, neutrons, and protons are present with a peak kinetic energies of ≈ 650, 250, and 180 MeV respectively. The presence of such flux highlights the need to consider modelling the treatment room environment when simulating therapeutic dose delivery.

CONCLUSION

Here, we have successfully shown that BDSIM is suited to simulating particle tracking in ion therapy accelerator models. Tracking has been validated through comparison to PTC in an in-house example medical beam line model. Particle losses and the subsequent energy deposition map shows that tracking secondary particles is particularly important for ions which undergo fragmentation in both the isocentre volume and in beam line materials. A range of secondary particle species were observed after a momentum cleaning collimator was modelled in a high dispersion region, all of which are all tracked in BDSIM. An increased secondary particle flux was observed due to interaction with the air between the gantry and phantom target. A flux of secondary particles exiting the phantom's rear surface emphasises the need to model the treatment room environment when simulating ion therapy beam lines. The recorded BDSIM sampler data can be easily transferred to other Monte Carlo tracking codes if required for comparison studies.

REFERENCES

[1] R. Atun *et al.*, "Expanding global access to radiotherapy", *The Lancet Oncology*, vol. 16, iss. 10, pp. 1153–1186, 2015.

[2] Cancer Research UK `www.cancerresearchuk.org`

ISBN: 978-3-95450-231-8 ISSN: 2673-5490 doi: 10.18429/JACoW-IPAC2023-THPM084

[3] N. R. Datta *et al.*, "Challenges and Opportunities to Realize "The 2030 Agenda for Sustainable Development" by the United Nations: Implications for Radiation Therapy Infrastructure in Low- and Middle-Income Countries", *Int J Radiat Oncol Biol Phys*, vol. 105, iss. 5, pp. 918-933, 2019.

[4] W. D. Newhauser *et al.*, *Physics in Medicine & Biology*, vol. 60, pp. R155–R209, 2015.

[5] A. Uzawa *et al.*, "Comparison of biological effectiveness of carbon-ion beams in Japan and Germany". *Int J Radiat Oncol Biol Phys*, vol. 73, iss. 5, pp. 1545-1551, 2009.

[6] H. Paganetti *et al.*, "Biological considerations when comparing proton therapy with photon therapy", *Sem. Rad. Onc.*, vol. 23, Iss. 2, pp. 77-87, 2013.

[7] H. X. Q. Norman *et al.*, "Review of tecnnologies for ion therapy accelerators", in *Proc. 12th Int. Particle Accelerator Conf. (IPAC'20)*, Campinas, SP, Brazil, 2021, pp. 2465–2468. doi:10.18429/JACoW-IPAC2021-TUPAB402

[8] C. Zeitlin *et al.*, "The Role of Nuclear Fragmentation in Particle Therapy and Space Radiation Protection", *Frontiers in Oncology*, vol. 6, 65, 2013.

[9] L.J. Nevay *et al.*, "BDSIM: An accelerator tracking code with particle-matter interactions", *Computer Physics Communications*, vol. 252, pp. 107200, 2020. doi:10.1016/j.cpc.2020.107200

[10] S. Agostinelli *et al.*, "Geant4 – A Simulation Toolkit", *Nucl. Instrum. Meth. A*, vol. 506, 2003.

[11] C. Hernalsteens *et al.*, "A novel approach to seamless simulations of compact hadron therapy systems for self-consistent evaluation of dosimetric and radiation protection quantities", *EPL*, vol. 132, 50004, 2020.

[12] E. Gnacadja *et al.*, "Optimization of proton therapy eye-treatment systems toward improved clinical performances", *Phys. Rev. Res.*, vol. 4, 013114, 2022.

[13] J. Yap *et al.*, "Beam characterisation studies of the 62 MeV proton therapy beamline at the Clatterbridge Cancer Centre", *Phys. Med.*, vol. 77, pp. 108-120, 2020.

[14] G. Aymar *et al.*, "LhARA: The Laser-hybrid Accelerator for Radiobiological Applications", *Frontiers in Physics*, vol. 8, 2020. doi:10.3389/fphy.2020.567738

[15] W. Shields *et al.*, "Hadron therapy machine simulations using BDSIM", in *Proc. 9th Int. Particle Accelerator Conf. (IPAC'18)*, Vancouver, BC, Canada, 2018, pp. 546–549. doi:10.18429/JACoW-IPAC2018-MOPML061

[16] J.M. Schippers *et al.*, "The SC cyclotron and beam lines of PSI's new proton therapy facility PROSCAN", *Nucl. Instr. Meth. B*, vol. 261, pp. 773–776, 2007.

[17] PSI Gantry 2 Lattice, http://aea.web.psi.ch/Urs_Rohrer/MyFtp, last visited 02 May 2023.

[18] E. Forest *et al.*, "Introduction to the Polymorphic Tracking Code", KEK, Japan, Rep. KEK-REPORT-2002-3, Jul 2002.

[19] *User's Reference Manual*, The Mad-X Program (Methodical Accelerator Design), CERN, Geneva, Switzerland, May 2021, pp. 1-266; http://madx.web.cern.ch/madx/releases/last-rel/madxuguide.pdf